Progress In Electromagnetics Research C, Vol. 117, 99–114, 2021

Compact Dual-Band Printed MIMO Antenna with Very Low Mutual Coupling for WLAN, Wi-MAX, Sub-6 GHz 5G and X-Band Satellite Communication Applications

Kommanaboyina V. Babu[1], Sudipta Das[2, *], Soufian Lakrit[3], Shobhit K. Patel[4, 5], Boddapati T. P. Madhav[6], and Hicham Medkour[7]

Abstract—In this paper, a dual-band modified multiple-input-multiple-output (MIMO) antenna with high isolation is presented and discussed. The proposed compact structure ($35 \times 25\,\text{mm}^2$) consists of two monopole elements and defected ground planes to obtain high impedance bandwidth. Two elliptical-shaped patches are placed orthogonal to each other to obtain high isolation, and a neutralization slit is integrated into the ground plane of each element to further improve the isolation between the elements. The measurement results of the proposed structure show satisfactory agreement with the simulation results. The measured bandwidths are 47.05% (2.6–4.2 GHz) and 64.72% (5.11–10 GHz) at $S_{11} \leq 10\,\text{dB}$ which covers bandwidth requirements of WiMAX (3.4–3.6 GHz, 5.25–5.85 GHz), sub 6 GHz 5G band (3.4–3.8 GHz), WLAN (5.15–5.35 GHz, 5.725–5.825 GHz), and X band satellite communication systems (7.25–8.39 GHz). The designed antenna offers a peak gain of about 9.0 dBi and radiation efficiency of about 92%. The measured minimum isolation is greater than 27.3 dB across the dual band with a maximum value of 73.4 dB. The envelope correlation coefficient (ECC) is below 0.0035, channel capacity loss less than 0.37 bits/s/Hz, and peak diversity gain about 10 dBi.

1. INTRODUCTION

The demand for multiple-input-multiple-output (MIMO) technology with high reliability and higher data rates has increased remarkably to fulfill the requirement of higher data rate throughput for current advanced wireless terminals or systems. MIMO antenna systems play a vital role in wireless communication systems to meet the requirements of omnidirectional characteristics, extra bandwidth, higher data rate, and limited space. So, the proper and well specified designs of MIMO antennas are a matter of important concern for these recent modern wireless systems such as Wireless Local Area Network (WLAN), Worldwide Interoperability for Microwave Access (Wi-MAX), and Fifth Generation (5G). The portable device terminals or hand held modern wireless communication systems occupy limited space due to their small size. To support these systems in terms of miniaturization, the multiple elements in the MIMO can be brought closer to make it miniaturized. However, while placing the elements closer, it becomes tough to maintain the desired envelope correlation coefficient and mutual coupling to ensure better isolation between the radiating patch elements, which destroys the entire

Received 2 October 2021, Accepted 8 December 2021, Scheduled 24 December 2021

* Corresponding author: Sudipta Das (sudipta.das1985@gmail.com).

[1] Department of Electronics and Communication Engineering, Vasireddy Venkatadri Institute of Technology, Guntur, India.

[2] Department of Electronics and Communication Engineering, IMPS College of Engineering and Technology, W.B., India.

[3] Mathematics and Information Systems Laboratory, EST of Nador, Mohammed First University, Oujda, Morocco. [4] Departmnt of Electronics and Communication Engineering, Marwadi University, Rajkot, Gujarat, India. [5] Computer Engineering Department, Marwadi University, Rajkot, Gujarat, India. [6] Department of Electronics and Communication Engineering, Koneru Lakshmaiah Education Foundation, Guntur, AP, India. [7] Department of Electronics, Faculty of Technology, Ferhat Abbas University Setif 1, Setif 19000, Algeria.

MIMO performance. The mutual coupling and arrangement of space between the elements are always inversely proportional to each other. On the other hand, one of the challenges of the multiple modern wireless systems is the design of dual band or multiband antennas to cover the several allocated frequency bands for many different wireless applications with a satisfactory performance at all frequency bands. The application of dual band antennas with wide impedance bandwidths eliminates the usage of separate multiple antennas and thus makes the implemented equipment smaller, lighter, and cheaper by reducing the space, weight, and cost constraints of the intended applications. Therefore, it becomes a very challenging task to design a compact dual-band/multiband MIMO antenna system with wide bandwidths, high gain, high efficiency, and better diversity performance while maintaining adequate isolation between the elements. In literature, researchers have proposed different design approaches for MIMO antennas to obtain these mentioned stringent design requirements. They have proposed many design techniques for single band [1–10] and dual band MIMO antennas [11–23]. The design methods include tapered radiating slot based 4 element MIMO antenna [1], broadband 4 element MIMO antenna using the combination of meander dipole, concave parabolic reflector, parasitic strip [2], 2 element MIMO antenna with G-shaped radiators, modified ground plane [3], CSRR loaded 4 element MIMO antenna [4], 4 element MIMO antenna with inverted L-shaped monopoles connected with common ground plane [5], 4 element MIMO antenna with orthogonally placed monopoles and decoupling structure composed of a circular patch and L-shaped branches [6], annular slot based MIMO antenna [7], stepped impedance resonator (SIR) based 8 element MIMO antenna [8], 2 element circular MIMO antenna with disc shaped wideband neutralization slot [9], 2 element MIMO antenna with grounded branch F-shaped monopole and neutralization line [10], metamaterial loaded dual band 2 element MIMO antenna for LTE and WLAN applications [11], 2 element 4-shaped MIMO antenna with microstrip matching network and DGS [12], inverted F-shaped 2 element MIMO antenna with decoupling devices for WLAN application [13], pentagonal shaped 4 element offset MIMO antenna with a T-shaped isolator [14], CPW-fed sunflower shaped fractal 2 element MIMO antenna [15], CPW-fed RSRR loaded 2 element MIMO antenna with ITI shaped isolation structure [16], double monopole structures with a meandering line decoupling resonator connected to the ground plane [17], 2×2 MIMO antenna with G-shaped elements and partially stepped ground [18], split ring resonator based 4 element MIMO antenna with interconnected ground plane [19], 2 element MIMO antenna with stub resonator and T-shaped monopoles [20], 8 element MIMO antenna with grounding branch [21], 2 element MIMO antenna with modified T-shape resonator with a rectangular loop [22], and 2 element MIMO antenna with orthogonally arranged antenna elements [23]. However, none of these MIMO designs provide all the combined characteristics with superior values to the best of the authors' knowledge, and for this reason, the authors of this paper have developed a new simple MIMO antenna with significant improvement in all the required characteristics.

This paper aims at designing a simple novel MIMO antenna with compact size, dual wide operating band, high isolation, high gain, high efficiency, and better MIMO performance parameters such as envelope correlation coefficient (ECC), total active reflection coefficient (TARC), diversity gain (DC), and mean effective gain (MEG). The proposed two-element MIMO antenna has a compact size of $35 \times 25\,\text{mm}^2$. Two ellipse-shaped orthogonally placed monopole antennas are selected as antenna elements. The proposed antenna has two wide operating bands, 2.6–4.2 GHz and 5.11–10 GHz with a peak gain of about 9 dBi and 92% radiation efficiency. The measured isolation is upto 73.4 dB. The ECC is below 0.0035, channel capacity loss less than 0.37 bits/s/Hz, and peak diversity gain about 10 dBi.

The novelties and benefits of the proposed design are as follows:

(i) **Less design complexity and cost-effective:** The suggested MIMO antenna is designed using a low cost easily available FR-4 substrate designed using two monopole radiators with a defected ground plane structure, and no additional decoupling structure is involved in the design process. So, the proposed antenna is much more cost-effective, and implementation is easy compared to reference works [1–23].

(ii) **Dual wide operating bands:** The proposed antenna offers dual wide band performance due to its monopole configuration and the presence of DGS. The −10 dB impedance bandwidths are about 1600 MHz (2.6–4.2 GHz) and 4890 MHz (5.11–10 GHz) at dual operating bands which cover bandwidth requirements of WiMAX (3.4–3.6 GHz, 5.25–5.85 GHz), sub 6 GHz 5G band (3.4–

3.8 GHz), WLAN (5.15–5.35 GHz, 5.725–5.825 GHz), and X band satellite communication systems (7.25–8.39 GHz). So, the proposed MIMO structure offers dual band operation in very compact size and better performance than other single band MIMO structures [1–10] and also much better impedance bandwidths at dual operating bands covering more wireless applications than other dual band antennas in the literature [11–23].

(iii) **Compact size:** The proposed configuration has a compact dimension of only $35 \times 25\,\text{mm}^2$ which is lower than the reference works in the literature [1–23].

(iv) **High gain and efficiency:** The proposed antenna offers a peak gain of about 9 dBi and radiation efficiency of about 92% due to the presence of neutralization slits in the modified ground plane, which are higher than other MIMO designs [1–23].

(v) **High Isolation:** The proposed antenna has obtained high isolation up to 73.4 dB without involving any extra parasitic or isolation structure between the antenna elements. The high isolation is achieved by adjusting the spacing between the orthogonally placed antenna elements and utilizing a neutralization slit in the ground plane of each element. The achieved isolation is much better than ref. works [1–23] in literature.

(vi) **Better MIMO performance parameters:** The proposed 2 element MIMO antenna offers better MIMO performance in terms of ECC, diversity gain, TARC, and channel capacity loss than the state of the art [1–23].

The work is supported by analytical modeling as well as simulation and practical measurements. The rest of the paper is organized as follows. In Section 2, the design and development of the proposed MIMO structure are presented in detail. In Section 3, the practical prototype and measurement results are explained verifying the simulated results. In Section 4, the MIMO diversity performance parameters of the proposed structure are presented and discussed in detail. Finally, in the last section before the conclusion, the performance of the proposed MIMO is compared with other reported MIMO designs.

2. DESIGN AND DEVELOPMENT OF THE PROPOSED ANTENNA

2.1. Geometry of the Proposed Antenna

The geometrical representations of the elliptical-shaped patches and corresponding modified ground plane of the proposed dual-band MIMO antenna are shown in Fig. 1. The proposed MIMO antenna has been designed using an FR4 substrate having $\tan\delta = 0.02$, thickness = 1.6 mm, and $\varepsilon_r = 4.4$. The MIMO antenna elements consist of elliptical-shaped radiators with a spacing of 3 mm between the radiating patches and excited by a microstrip feed line. For achieving the dual band characteristics with wide impedance bandwidths, a small rectangular monopole ground plane is used with two modified curved wings and a central rectangular cut at the upper edge of the ground. The neutralization line in

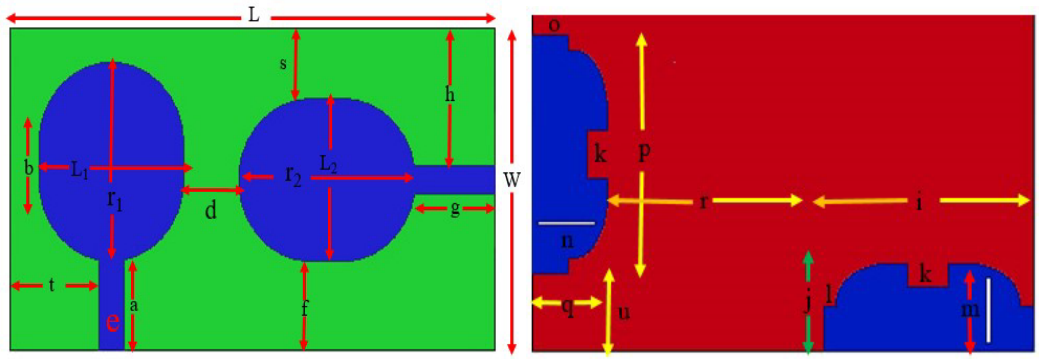

Figure 1. Structure of the proposed MIMO antenna, (a) elliptical patches (top view), (b) modified ground plane (bottom view).

the form of a rectangular slit is introduced on the right side of each ground plane to improve the isolation between antenna elements and to enhance the radiation performance (gain and radiation efficiency) of the proposed MIMO antenna. The related details corresponding to the dimensions of the proposed elliptical MIMO antenna are indicated in Table 1.

Table 1. Elliptical shape MIMO design dimensions are in mm.

Parameter	L	W	r_1	a	b	L_1	d	e	f	g	h	i	j
Dimensions (mm)	35	25	9	10	2.4	13	3	3	5.5	10	10.5	18	2.4
Parameter	L_2	k	l	m	n	O	P	q	r	s	t	u	r_2
Dimensions (mm)	13	4	1.6	2.2	1.8	2	18	2.4	9.3	3.4	9	2.5	6

2.2. Design Evolution Stages of the Proposed Antenna

The evolution stages for designing of a single antenna element are shown in Fig. 2. The structural views of the front and back planes of the single element antenna along with variations in corresponding

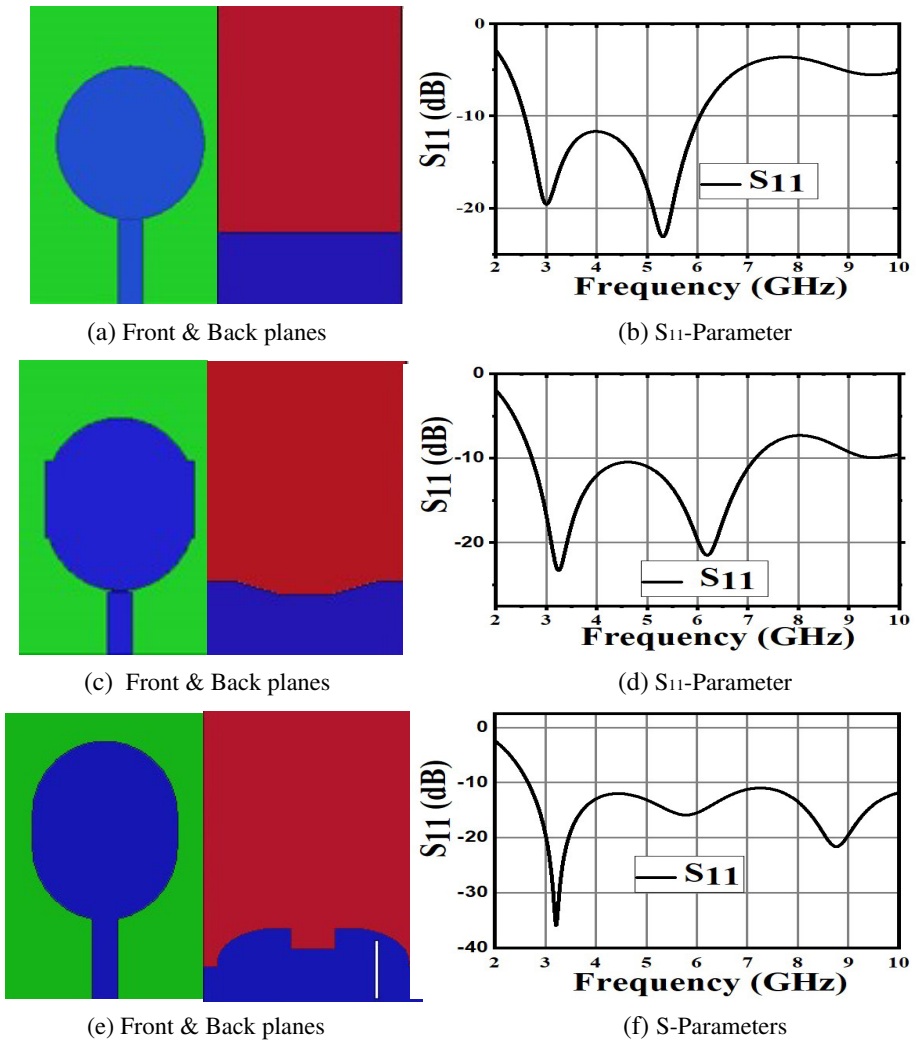

(a) Front & Back planes (b) S11-Parameter

(c) Front & Back planes (d) S11-Parameter

(e) Front & Back planes (f) S-Parameters

Figure 2. Evolution stages of single antenna design.

reflection coefficients (S_{11} parameters) for each design stage are demonstrated in Figs. 2(a)–(f). The working mechanism of the antenna antenna element is discussed with the help of its resonance characteristics curves. The single antenna element with circular patch and simple rectangular ground plane offers good impedance matching characteristics over the frequency band ranging from 2.8 to 6.0 GHz [see Fig. 2(b)]. In the next design step, due to the modifications in its geometry as shown in Fig. 2(c), the antenna operates from 2.9 to 7.0 GHz for $S_{11} \leq 10$ dB with slight shifts in the resonant frequencies. Then finally the shape of the patch is transformed to an elliptical shape, and the ground plane is defected with rectangular slots as depicted in Fig. 2(e). As observed in Fig. 2(f), the higher resonant frequency is prominently shifted near 9 GHz, and further enhancement in operating bandwidth is noticed with the best impedance matching. The obtained results indicate the bandwidth coverage of several wireless applications such as WiMAX (3.4–3.6 GHz, 5.25–5.85 GHz), sub 6 GHz 5G band (3.4–3.8 GHz), WLAN (5.15–5.35 GHz, 5.725–5.825 GHz), and X band satellite communication systems (7.25–8.39 GHz).

Now, to support the claimed wireless applications with enhanced data rate throughput under the applicable conditions of interference, fading, and multipath, the single antenna element has been transformed into MIMO configuration to provide good diversity characteristic parameters and high isolation. The design evolution stages to obtain the proposed structure of the dual band MIMO antenna with good impedance matching and high isolation characteristics are shown in Fig. 3. The corresponding simulated results (S_{11} and S_{21} parameters) of the different design step by step wise analyses are depicted in Figs. 4 and 5, respectively.

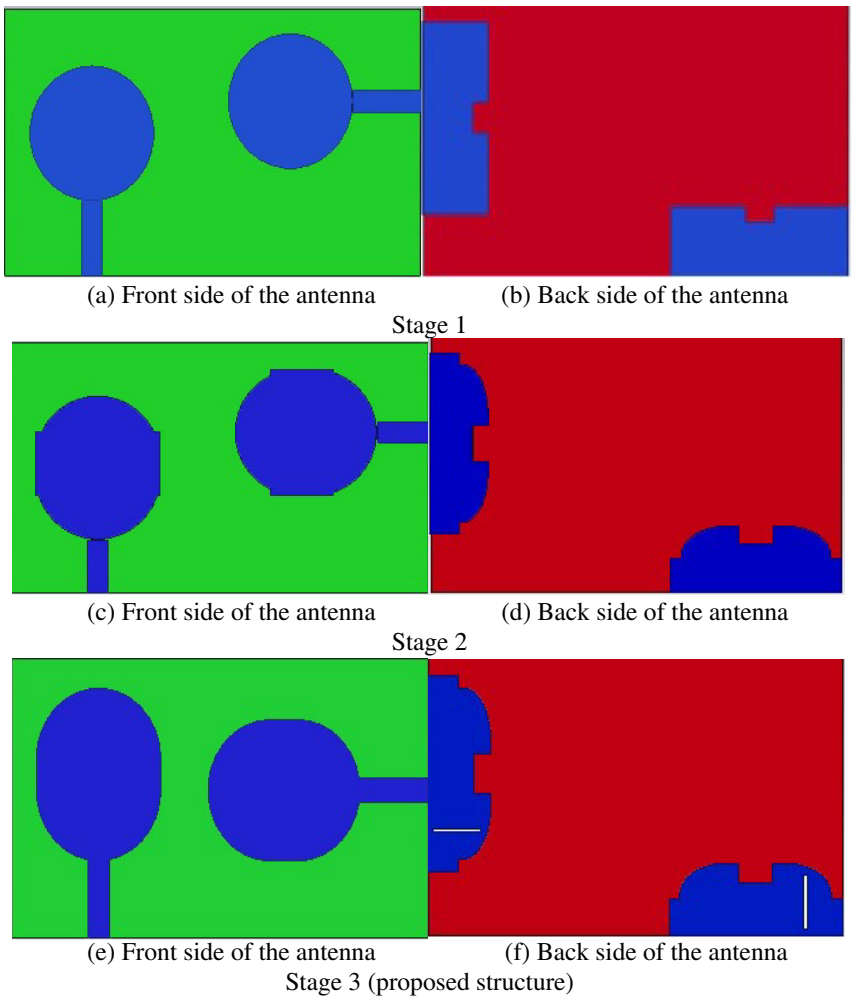

Figure 3. Stage wise design evolution of the proposed MIMO antenna.

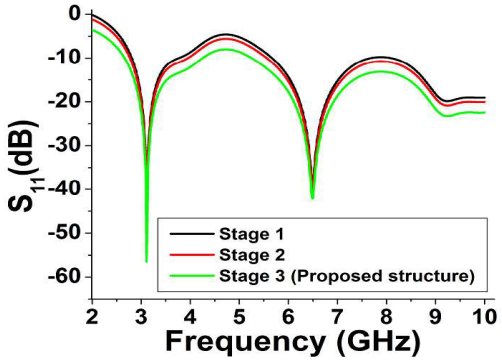

Figure 4. S_{11} parameter for different stages.

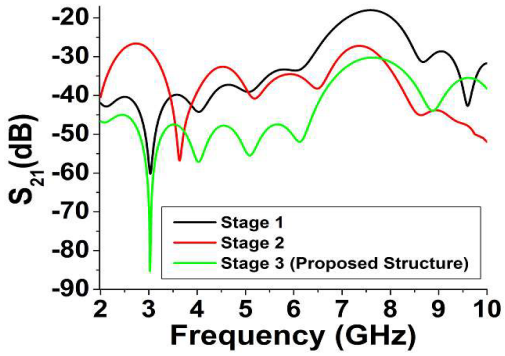

Figure 5. S_{21} parameters for different stages.

In stage 1, the designed structure is composed of a basic circular-shaped patch connected to the rectangular strip and a small rectangular cut at the rectangular monopole ground plane to achieve dual wideband operation. As observed from reflection coefficient characteristics shown in Fig. 4 (stage 1), the designed antenna offers dual band operation with −10 dB impedance bandwidth (IBW) of about 910 MHz (2.81–3.72 GHz) for the lower band and 4330 MHz (5.67–10 GHz) for the upper band but does not fulfill the bandwidth requirements for a few intended applications WiMAX (5.25–5.85 GHz), sub 6 GHz 5G band (3.4–3.8 GHz), and WLAN (5.15–5.35 GHz). In stage 2, the designed antenna offers maximum return loss $|S_{11}|$ of about 53 dB at the resonant frequency (3.1 GHz) of the lower band and 38 dB at the resonant frequency (6.5 GHz) of the upper band. The transmission coefficient characteristics (Fig. 5) for stage 1 reveal more than 18 dB isolation value between the antenna pairs. In the second stage of the design, the patches are transformed to elliptical shape, and modified curvature wings are added on both sides of the monopole ground plane to achieve better impedance matching and improved isolation at the dual operating bands. The S_{11} for stage 2 of the design evolution shows a noticeable improvement in operating bandwidth offering (2.78–3.95 GHz) for the lower band which covers the frequency band (3.4-3.8 GHz) of sub 6 GHz 5G applications and (5.57–10 GHz) for the upper band with better return loss $|S_{11}|$ characteristics. This structure also offers an improvement in the isolation level which implies a reduction in the mutual coupling between the pair of patches due to the presence of modified curved wings in the ground plane. The suggested structure at this stage offers isolation ($|S_{21}|$) greater than 26 dB but still incapable to support WiMAX (5.25–5.85 GHz) and WLAN (5.15–5.35 GHz) due to insufficient operating bandwidth. Finally, in stage 3, the structure of the proposed antenna has been presented which offers much better impedance matching, operating bandwidth, and isolation. In the final stage, the position of the horizontally placed patch is slightly shifted, and the neutralization line in the form of the slit is introduced on the right sides of each monopole ground plane to reduce the mutual coupling to a great extent compared to the previous design stages. This structure offers an enhancement in operating bandwidths by 420 MHz for the lower band (2.66–4.25 GHz) with an improvement in the return loss. The higher operating frequency band gets broadened by 430 MHz, and the achieved band ranges from 5.14 to 10 GHz for $S_{11} \leq -10$ dB which supports the bandwidth requirements of Wi-MAX (5.25–5.85 GHz) and WLAN (5.15–5.35 GHz) applications. The proposed configuration also shows a remarkable reduction in mutual coupling offering a minimum isolation value ≥ 30 dB for the operating bands. The achieved isolation is very attractive and satisfies the considerable limit for desired practical wireless applications. The detailed results of the analysis are summarized in Table 2. It can be observed that the proposed configuration offers sufficient bandwidth to support all the intended wireless applications with maximum suppression level of mutual coupling or the highest level of isolation for MIMO systems.

2.3. Effect of Spacing 'd' between Patches on the Response of the Proposed Antenna

The variations of the inter-element distance between the patches have a significant effect on the resonance characteristics of the antenna. Fig. 6 depicts the variations of the S_{11} parameter as a function of changes in the dimension of spacing between the patches. The operating bandwidth remains the same,

Table 2. Simulated results at different stages of structural development.

Antenna design Stages	Operating bands	IBW ($S_{11} \leq -10$ dB) (MHz)	Bandwidth (%)	Peak Gains (dBi)	Radiation Efficiency (%)	Minimum isolation ($\lvert S_{21}\rvert$)
Stage # 1 (Circular patch+Defected rectangular monopole ground plane)	Lower band	910 (2.81–3.72 GHz)	27.87	4.17	30	> 18 dB
	Upper band	4330 (5.67–10 GHz)	55.26	2.98	60.4	
Stage # 2 (Elliptical patch+Defected monopole ground plane with curved wings)	Lower band	1170 (2.78–3.95 GHz)	34.76	4.97	81.4	> 26 dB
	Upper band	4430 (5.57–10 GHz)	56.90	3.51	82	
Stage # 3 (Elliptical patch+Defected monopole ground plane with curved wings+ Neutralization slits)	Lower band	1590 (2.66–4.25 GHz)	46.02	7.9	92	> 30 dB
	Upper band	4860 (5.14–10 GHz)	64.20	9.0	84	

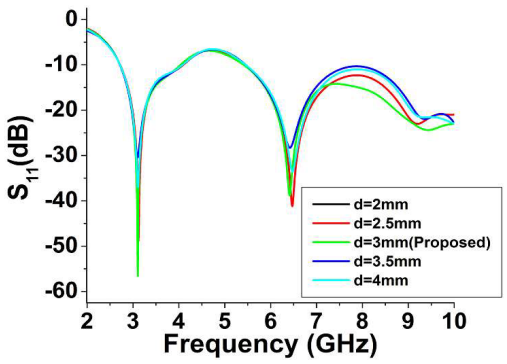

Figure 6. Effect of element spacing 'd' on S_{11}.

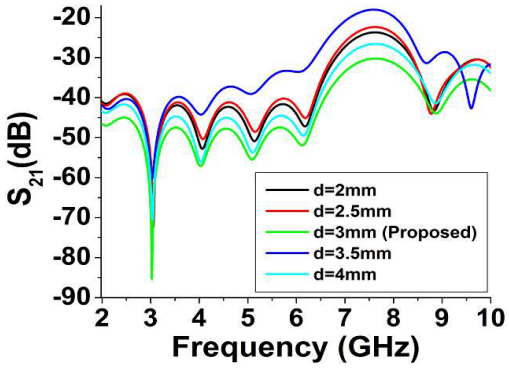

Figure 7. Effect of element spacing 'd' on S_{21}.

but improvement in terms of impedance matching is noticed due to variations in element spacing. It is observed that the maximum return loss is about 58 dB, and hence better impedance matching is obtained for the proposed value of the spacing parameter 'd'. The variations of transmission coefficients (S_{21}) parameter for various distances between the patches are shown in Fig. 7. The effect of element spacing on mutual coupling reduction between the pair of patches is very prominent. For the proposed distance $d = 3$ mm, a great improvement in isolation is observed; the suggested MIMO antenna delivers minimum isolation of 30 dB; and the maximum level has reached 85 dB. Table 3 summarizes the S-parameters (S_{11} and S_{21}) for different spatial dimensions between the patches.

Table 3. Comparison of S-Parameters for different distances between the antennas.

Distance between antennas (mm)	Maximum return loss $\|S_{11}\|$ (dB)	Minimum isolation $\|S_{21}\|$ (dB)	Maximum isolation $\|S_{21}\|$ (dB)
$d = 4$	40	26.5	70.4
$d = 3.5$	30	18	60
$d = 3$ **(proposed)**	58	30	85
$d = 2.5$	48	22.3	72.3
$d = 2$	36	23.7	70.3

2.4. Analysis of the Proposed MIMO Antenna Structure

The antenna elements are placed in perpendicular arrangement for the proposed MIMO configuration. For this reason, the characteristic impedance of the proposed antenna geometry changes due to the generation of excited modes with their corresponding differential distribution of surface currents. Figs. 8(a)–(h) show the surface current distribution of dual band elliptical MIMO antenna at 3.1 GHz & 6.5 GHz at the two ports. The maximum current is concentrated near the strip of the elliptical shape, and it is also observed that maximum current at the resonant frequencies can be produced by considering the defect in the ground plane depending on the port excitement. From the current distribution at the ground plane, it can be observed that current density is much stronger at the upper edge of the ground plane and mainly at the rectangular cut. The rotation of elliptical-shaped patches excites the corresponding resonant modes to the dominant mode which results in higher frequency bands. The elliptical shape MIMO design resonant frequency f_{ri} can be evaluated as

$$f_{ri} = \frac{c}{2\,L_i\,\sqrt{\varepsilon_{r,eff}}} \tag{1}$$

where ε_{reff} is the effective dielectric constant of the substrate, 'c' the free space velocity of light, and L_i the average length of the elliptical patch.

The elliptical patch length L_i can be evaluated as

$$L_i = \{\pi(A_{r_i} + B_{r_i}) - k\}; \quad i = 1, 2 \tag{2}$$

where A_{r_i} and B_{r_i} represent major and minor axes of the elliptical shape.

3. PRACTICAL PROTOTYPE, RESULTS, AND DISCUSSION

3.1. *S*-Parameters and Radiation Characteristics

Figure 9 shows the fabricated prototype of the proposed dual-band MIMO antenna. The measurements of S-parameters are obtained by one of the ports (port # 1) excited, and another port of the antenna is (port # 2) terminated by the characteristic impedance of 50 Ω load and vice versa. The comparison of the measured and simulated results (S_{11} and S_{21}) is depicted in Fig. 10. A reasonable agreement is observed between the simulated and measured results. However, the few discrepancies are probably due to imperfections in the fabrication process, soldering effect, losses associated with the material, SMA connectors, and feed cable. The measured results validate the design concept and show dual band operation with −10 dB bandwidth of 1600 MHz (2.6–4.2 GHz) and 4890 MHz (5.11–10 GHz) respectively for the lower and higher bands. It is clear from the measured result shown in Fig. 10 that the proposed antenna has a minimum isolation of 27.3 dB across the dual band. The comparison of simulated and measured radiation patterns of the proposed antenna at dual band frequencies revealing its co- and cross-pol components in E-field and H-field planes is shown in Figs. 11(a)–(b). Due to the identical nature of the two elements of the designed MIMO structure, radiation patterns are also almost identical for $\varphi = 0°$. Therefore, radiation pattern measurements at only port 1 are considered here. The co-polarization radiation patterns at 3.1 GHz are similar to a figure of 8 in both xz and yz planes. The

co-polarization radiation patterns in 6.5 GHz are omnidirectional with slight distortion due to the use of monopole configuration of the ground planes. Due to the defect in the ground plane, the radiation patterns degrade the system performance at dominant frequencies, and the dominant excited modes produce uneven current distributions perturbations. The cross polarization is very low for all the presented results. It is observed that measured and simulated co-polarized radiation patterns are in good agreements. The radiation efficiency and gain of the proposed antenna are shown in Fig. 12. The

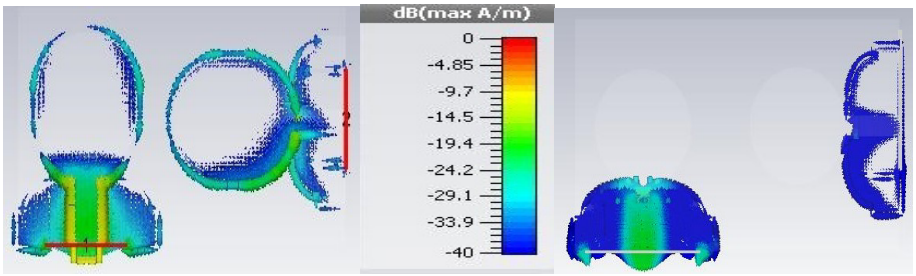

(a) 3.1 GHz port 1 excited (patch) (b) 3.1 GHz port 1 excited (ground plane)

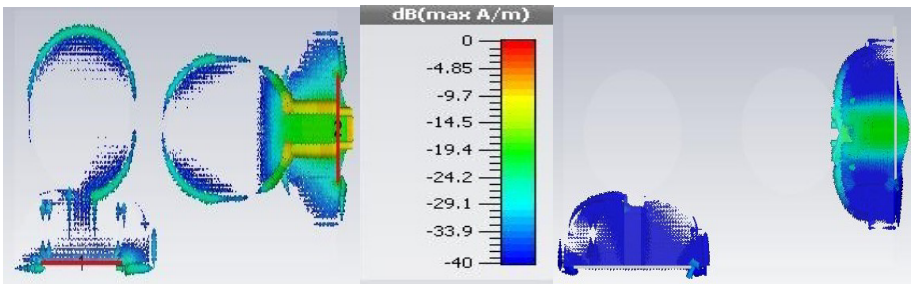

(c) 3.1 GHz port 2 excited (patch) (d) 3.1 GHz port 2 excited (ground plane)

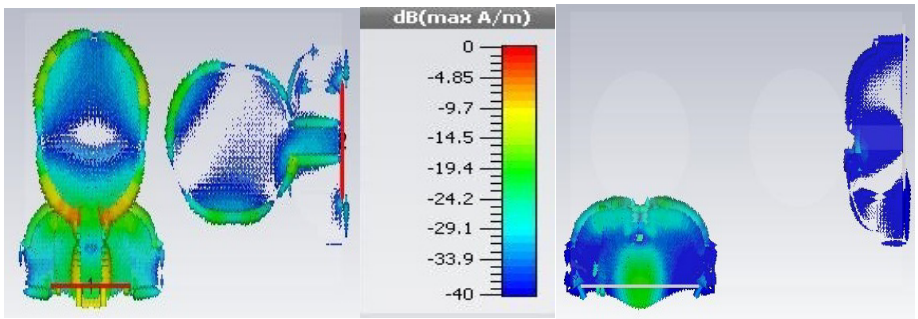

(e) 6.5 GHz port 1 excited (patch) (f) 6.5 GHz port 1 excited (ground plane)

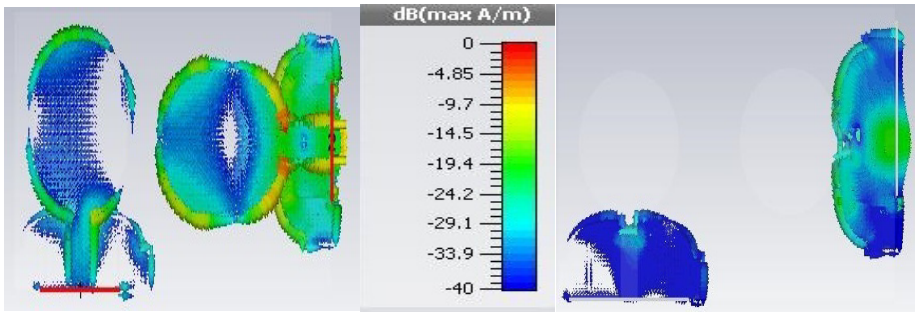

(g) 6.5 GHz port 2 excited (patch) (h) 6.5 GHz port 2 excited (ground plane)

Figure 8. Surface current distribution of the dual band MIMO antenna.

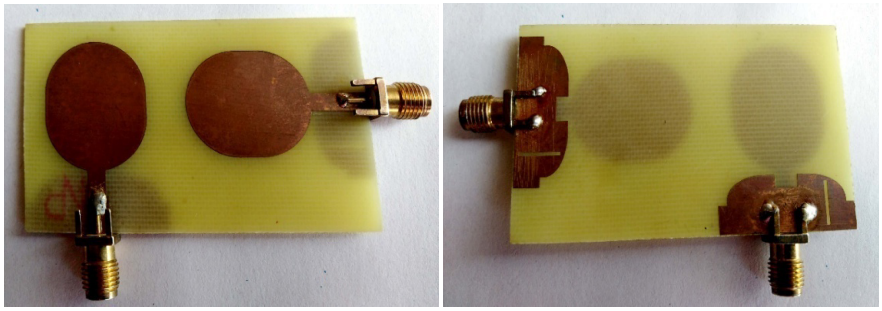

(a) (b)

Figure 9. Prototype of the proposed MIMO antenna, (a) front side, (b) back side.

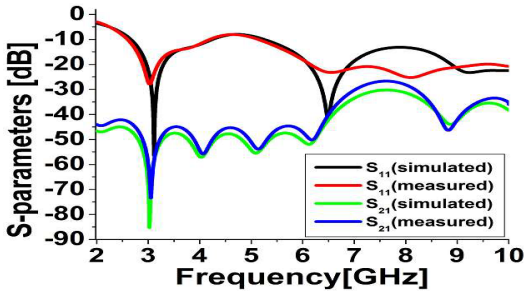

Figure 10. *S*-Parameters comparison of the proposed MIMO antenna.

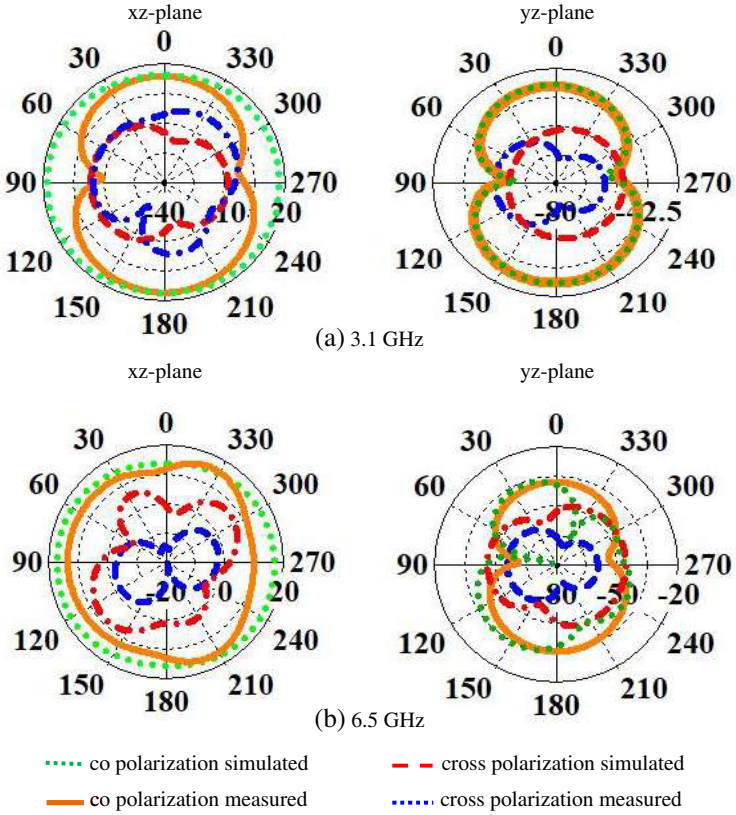

Figure 11. Radiation patterns of the proposed MIMO antenna, (a) 3.1 GHz, (b) 6.5 GHz.

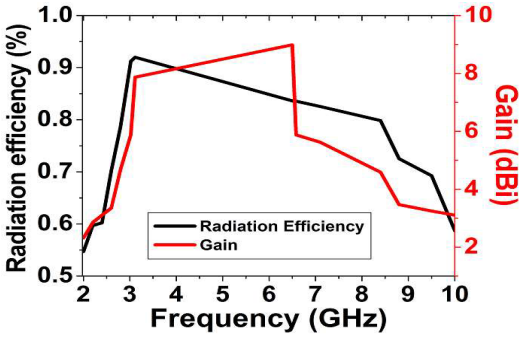

Figure 12. Radiation efficiency (%) and Peak gain (dBi) Vs. Frequency.

gain of the proposed MIMO antenna is measured with the support of a driving software system using a turn-table mechanism setup. For the measurement of gain, a horn antenna with known gain is used as the primary antenna (reference antenna), and the proposed antenna is used as the secondary antenna [antenna under test (AUT)]. In the measurement process, the gain of the proposed antenna (AUT) is calculated by direct comparison method. As shown in the figure, and the simulated radiation efficiencies are around 92% and 84% respectively at the dual band resonant frequencies 3.1 GHz and 6.5 GHz. The simulated peak gains for the resonant frequencies of the lower and upper bands are around 7.9 dBi and 9 dBi, respectively.

4. MIMO DIVERSITY PERFORMANCE PARAMETERS

MIMO antenna diversity performance parameters, channel capacity, envelope correlation coefficient (ECC), diversity gain (DG), total active reflection coefficient (TARC), and mean effective gain (MEG), have been studied in this section.

4.1. ECC (Envelope Correlation Coefficient) and DG (Diversity Gain)

The value of ECC in MIMO radiator analysis is used to indicate the amount of correlation between the adjacent antenna elements. The value of ECC must be less than 0.5 to ensure better diversity performance between the adjacent antenna elements of a MIMO design for wireless applications [24]. For the N-port system, the ECC between the elements of i and j can be evaluated by the relation [25] given in Equation (3).

$$\rho_e(i,j,N) = \left| \frac{\sum_{n=1}^{N} S_{i,n}^{*} S_{n,j}}{\left| \prod_{k=i,j} \left(1 - \sum_{n=1}^{N} S_{K,n}^{*} S_{n,K} \right) \right|^{1/2}} \right|^2 \tag{3}$$

The ECC for a two-port system, $i = 2$, $j = 2$ and $N = 2$ is expressed by Equation (4).

$$\rho_e(1,1,2) = \frac{\left| S_{11}^{*} S_{12} + S_{21}^{*} S_{22} \right|^2}{(1 - |S_{11}|^2 - |S_{21}|^2)(1 - |S_{11}|^2 - |S_{21}|^2)} \tag{4}$$

The parameter diversity gain (DG) indicates an improvement in MIMO performance. It is computed by the relation [26] given in Equation (5).

$$DG = 10\sqrt{1 - |\rho_c|^2} \tag{5}$$

The variations of ECC and DG for the designed dual band elliptical-shaped MIMO antenna are shown in Fig. 13. The ECC values are below 0.0035 in the working frequency bands of the proposed MIMO,

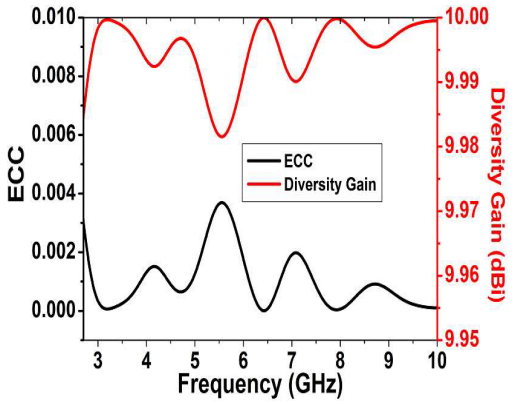

Figure 13. ECC and Diversity gain Vs. Frequency.

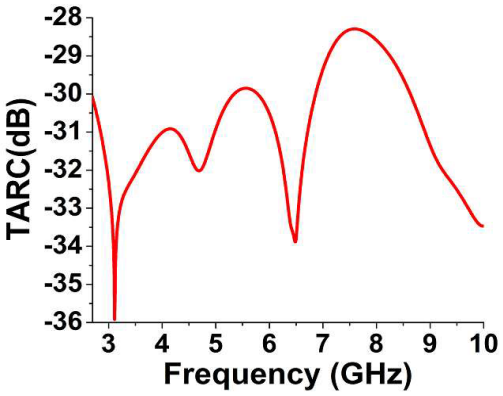

Figure 14. TARC Vs. Frequency.

which suggests very good radiation diversity performance. As observed in Fig. 12, the diversity gain is greater than 9.98 dBi throughout the operating bands of the proposed MIMO antenna.

4.2. TARC (Total Active Reflection Coefficient)

TARC is defined as the ratio of the square root of total reflected power and total incident power for the overall MIMO system of the antenna [27]. Generally, the presence of multiple antenna elements influences the performance parameters in a MIMO system. So, it is essential to compute the TARC as it measures the behavior of the affected system and provides a complete characterization of the effectiveness of the MIMO system. The TARC within acceptable value accounts for mutual coupling and also signifies the non-variance of resonance characteristics (resonant frequency and impedance bandwidth).

Total active reflection coefficient (TARC) is obtained by using the relation given in [28] shown in Equation (6).

$$TARC = \sqrt{|S_{11} + S_{12}e^{j\theta}|^2 + |S_{21} + S_{22}e^{j\theta}|^2} \Big/ \sqrt{2} \tag{6}$$

Here the value of θ lies between 0 and 2π.

Figure 14 indicates the response of TARC for the proposed dual-band MIMO structure. The acceptable value of TARC for any MIMO design is less than 0 dB. For the proposed MIMO, it is better than -28 dB for the entire operating bandwidth which is well accepted for practical applications.

4.3. CCL (Channel Capacity Loss)

CCL indicates the highest limit up to which the information in bits/s/Hz can be transferred without a significant loss, and for a well designed MIMO, its value should be less than 0.4 bits/s/Hz [29]. It can be evaluated using Equation (7). For the proposed MIMO antenna, the channel capacity loss is less than 0.37 bits/s/Hz which confirms a better data transmission rate without any additional power requirement.

$$C_{loss} = -\log_2 \det(\Psi^R) \tag{7}$$

$$\Psi^R = \begin{pmatrix} \rho_{11} & \rho_{12} \\ \rho_{21} & \rho_{22} \end{pmatrix} \tag{8}$$

where,

$$\rho_{ii} = 1 - \left(|S_{ii}|^2 + |S_{ij}|^2\right), \text{ and } \rho_{ij} = -\left(s^*_{ii}\, S_{ij} + s^*_{ij}\, S_{jj}\right), \quad for\ i, j = 1\ or\ 2 \tag{9}$$

where Ψ^R indicates the receiving antenna correlation matrix.

For any MIMO analysis the channel capacity (C) is computed by Equation (10) which indicates the amount of acceptable bandwidth of the channel.

$$C = \log_2 \left(\det \left(1 + \frac{SNR}{M} HH' \right) \right) \tag{10}$$

The above mentioned MIMO performance parameters are summarized in Table 4 for the proposed dual band MIMO antenna.

Table 4. MIMO parameters of the proposed dualband antenna.

Resonant Frequency (GHz)	Correlation Coefficient (ρ)	ECC	TARC (dB)	DG	Channel Capacity (bits/sec/Hz)	Channel Capacity Loss in (bits/sec/Hz)
3.1	0.000476	0.000106	−34.74	10	3.283	0.37
6.5	0.000463	0.000075	−33.67	10	3.985	0.31

4.4. MEG (Mean Effective Gain)

Another important parameter required for the characterization of the MIMO antenna in a multipath environment is the mean effective gain. It evaluates the gain of each element while considering the propagation effects, antenna total efficiency, and radiation power pattern effects. It can be evaluated by using [30] Equation (11)

$$MEG = \int_0^{2\pi} \int_0^{\pi} \left[\frac{XPR}{1+XPR} G_\theta(\theta,\phi) P_\theta(\theta,\phi) + \frac{1}{1+XPR} G_\phi(\theta,\phi) P_\phi(\theta,\phi) \right] \sin\theta d\theta d\phi \tag{11}$$

The above equation satisfies

$$\int_0^{2\pi} \int_0^{\pi} [G_\theta(\theta,\phi) + G_\phi(\theta,\phi)] \sin\theta d\theta d\phi = 4\pi \tag{12}$$

$$\int_0^{2\pi} \int_0^{\pi} P_\theta(\theta,\phi) \sin\theta d\theta d\phi = \int_0^{2\pi} \int_0^{\pi} P_\phi(\theta,\phi) \sin\theta d\theta d\phi = 1 \tag{13}$$

$$XPR = \frac{P_V}{P_H} \tag{14}$$

Here, $XPR =$ Cross polarization ratio.

P_θ and P_φ are the θ and φ components of incident power angular density functions. G_θ and G_φ are the θ and φ components of power gain patterns of the antenna. The MEG of the proposed dual band MIMO antenna is evaluated for both isotropic and gaussian media at $XPR = 0\,\text{dB}$ and $XPR = 6\,\text{dB}$ as listed in Table 5.

Table 5. Mean Effective Gains (MEGs) for the proposed dual-band MIMO antenna.

Frequency (GHz)	Isotropic Medium		Gaussian Medium	
	MEG (XPR @ 0 dB)	MEG (XPR @ 6 dB)	MEG (XPR @ 0 dB)	MEG (XPR @ 6 dB)
3.1	−2.992	−4.7577	−3.5849	−6.6986
6.5	−2.989	−4.2204	−3.6796	−6.0880

Table 6. Comparison of the proposed design with some other MIMO antennas.

Ref.	Size (mm^2)	No. of Elements	Operating Bands (GHz)	Isolation (dB)	Peak gain (dBi)	Radiation Efficiency (%)	Isolation improvement method	ECC
[1]	66×66	4	2.3–2.7	> 17	3.67	NR	Cross shaped stubs	< 0.04
[2]	85×85	4	2.32–2.95	> 17	5.5	NR	Parasitic strip	NR
[3]	50×50	2	2.26–6.78	> 22.5	3.51	86.90	Ground branches	0.0059
[4]	100×50	4	2.40–2.80	> 12	0.8	NR	CSRR	< 0.3
[5]	40×40	4	2.70–4.94	> 11	4	NR	Common ground	< 0.1
[6]	30×30	4	4.58–6.12	> 15.4	4.8	67–82	Decoupling structure	< 0.15
[7]	120×60	2	3.8–2.45	> 10	2.43	73	Annular slot based	< 0.1
[8]	136×68	8	3.4–3.8	> 11.7	NA	NR	SIR Structure	< 0.1
[9]	35×33	2	3.1–5.0	> 22	3.8	75	Neutralization line	< 0.1
[10]	80×60	2	1.7–2.76	> 15	NA	83.4	Neutralization line	< 0.0040
[11]	180×90	2	2.4–3.1 5.1–5.8	> 27	6	NR	Metameterial	< 0.3
[12]	100×50	2	0.803–0.823 2.44–2.9	> 17	2.4	NR	DGS	< 0.21
[13]	77.5×52	2	2.4–2.48 5.15–5.825	> 15	2.6	82.00	Decoupling structure	< 0.2
[14]	65.3×65.3	4	2.24–2.64 3.41–3.69	> 12	4.52	71.00	T-shaped isolator	< 0.01
[15]	50×40	2	2.0–2.9 5.0–10.0	> 20	6	85.00	Inserting strip line	< 0.05
[16]	72×56	2	2.24–2.90 3.90–7.55	> 24	5.6	81.00	CPW	< 0.04
[17]	60×60	2	2.31–2.48 4.92–5.82	> 25.3	NA	NR	Meandering line	< 0.08
[18]	70×70	4	2.408–2.776 4.96–5.64	> 21	4.13	NR	PSG	< 0.004
[19]	48×70	4	2.2–3.5 5.2–5.8	> 15	4	89.55	SRR with common ground plane	< 0.018
[20]	50×26	2	2.35–2.65 4.9–6.2	> 20	4.7	82.3	Stub resonator	< 0.06
[21]	74×124	8	2.4–2.7 3.3–3.6	> 15.1	NA	80.00	Grounding branches	< 0.21
[22]	40×40	2	2.2–2.7 4.6–5.9	> 15	4.5	NR	Modified T shaped resonator	< 0.1
[23]	42×62	2	2.38–2.52 3.19–6.44	> 15	2.9	NR	Orthogonal placement of antenna	< 0.02
Proposed antenna	35×25	2	2.6–4.2 5.11–10	> 27.3	9.0	92	Neutralization slit	< 0.0035

ECC = Envelope Correlation Coefficient; NR = Not Reported

5. PERFORMANCE COMPARISON WITH OTHER MIMO ANTENNAS

The performance comparison analysis of the proposed dual band MIMO antenna with other reported MIMO designs is summarized in Table 6. The proposed design is highly attractive due to its more compact size and much better performance in terms of impedance bandwidth, gain, radiation efficiency, isolation, and ECC than other reported single band/dual-band MIMO antennas in the literature [1–23]. The proposed antenna shows dual wideband performance which covers the frequency band requirements of more various wireless applications such as WiMAX (3.4–3.6 GHz, 5.25–5.85 GHz), sub 6 GHz 5G band (3.4–3.8 GHz), WLAN (5.15–5.35 GHz, 5.725–5.825 GHz), and X band satellite communication systems (7.25–8.39 GHz) altogether than references [1–23]. Moreover, the suggested MIMO manifests efficient diversity performance offering acceptable values of low loss channel capacity, diversity gain, TARC, and MEG.

6. CONCLUSION

An ellipse-shaped compact dual band MIMO antenna system with high isolation between the antenna elements is presented. The dimension of the proposed MIMO antenna is only $35 \times 25\,\text{mm}^2$. The isolation is improved by introducing neutralization slits in the ground plane of the MIMO antenna system. The measured results show that the designed MIMO antenna operates in dual bands (2.6–4.2 GHz) and (5.11–10 GHz), having IBWs of 47.05% and 64.72%, respectively with isolation (S_{21}) greater than 27.3 dB for each working band. The proposed antenna shows stable radiation patterns with a peak gain of 9 dBi and maximum radiation efficiency of 92%. The antenna has ECC < 0.0035, diversity gain > 9.98 dB and channel loss capacity < 0.37 bits/sec/Hz, which assures better diversity performance. Hence, the proposed MIMO antenna is suitable for several wireless communication systems like WLAN, WiMAX, sub 6 GHz 5G band, and X band satellite communication systems.

REFERENCES

1. Yussuf, A. A. and S. Paker, "Design of a compact quad-radiating element MIMO antenna for LTE/Wi-Fi application," *AEÜ — Int. J. Electron. Commun.*, Vol. 111, 152893, 2019.
2. Ding, K., C. Gao, D. Qu, and Q. Yin, "Compact broadband MIMO antenna with parasitic strip," *IEEE Antennas and Wireless Propagation Letters*, Vol. 16, 2349–2353, 2017.
3. Xia, X.-X., Q.-X. Chu, and J.-F. Li, "Design of a compact wideband MIMO antenna for mobile terminals," *Progress In Electromagnetics Research C*, Vol. 41, 163–174, 2013.
4. Sharawi, M. S., A. B. Numan, M. U. Khan, and D. N. Aloi, "A CSRR loaded MIMO antenna system for ISM band operation," *IEEE Transactions on Antennas and Propagation*, Vol. 61, No. 8, 4265–4274, 2013.
5. Debdeep, S. and V. K. Srivastava, "A compact four-element MIMO/diversity antenna with enhanced bandwidth," *IEEE Antennas and Wireless Propagation Letters*, Vol. 16, 2469–2472, 2017.
6. Ming, Y. and J. Zhou, "A compact pattern diversity MIMO antenna with enhanced bandwidth and high-isolation characteristics for WLAN/5G/WiFi applications," *Microwave and Optical Technology Letters*, 1–12, 2020.
7. Rifaqat, H., A. Ghalib, and M. S. Sharawi, "Annular slot-based miniaturized frequency-agile MIMO antenna system," *IEEE Antennas and Wireless Propagation Letters*, Vol. 16, 2489–2492, 2017.
8. Shi, H., X. Zhang, J. Li, P. Jia, J. Chen, and A. Zhang, "3.6-GHz eight-antenna MIMO array for mobile terminal applications," *AEÜ — Int. J. Electron. Commun.*, Vol. 95, 342–348, 2018.
9. Zhang, S. and G. Pedersen, "Mutual coupling reduction for UWB MIMO antennas with a wideband neutralization line," *IEEE Antennas and Wireless Propagation Letters*, Vol. 15, 166–175, 2015.
10. Wang, Y. and Z. Dun, "A wideband printed dual-antenna system with a novel neutralization line for mobile terminals," *IEEE Antennas and Wireless Propagation Letters*, Vol. 12, 1428–1431, 2013.
11. Rezvani, M. H. and Z. Yashar, "A dual-band multiple-input multiple-output microstrip antenna with metamaterial structure for LTE and WLAN applications," *AEÜ — Int. J. Electron. Commun.*, Vol. 93, 277–282, 2018.

12. Sharawi, M. S., A. B. Numan, M. U. Khan, and D. N. Aloi, "A dual-element dual-band MIMO antenna system with enhanced isolation for mobile terminals," *IEEE Antennas and Wireless Propagation Letters*, Vol. 11, 1006–1009, 2012.
13. Deng, J. Y., J. Y. Li, L. Zhao, and L. Guo, "A dual-band inverted-F MIMO antenna with enhanced isolation for WLAN applications," *IEEE Antennas and Wireless Propagation Letters*, Vol. 16, 2270–2273, 2017.
14. Leeladhar, M., M. V. Kartikeyan, and R. K. Panigrahi, "Offset planar MIMO antenna for omnidirectional radiation patterns," *International Journal of RF and Microwave Computer Aided Engineering*, Vol. 28, No. 6, e21274, 2018.
15. Amer, T. A., "Novel sunflower MIMO fractal antenna with low mutual coupling and dual wide operating bands," *International Journal of Microwave and Wireless Technologies*, 1–9, doi.org/10.1017/S1759078719001375.
16. Kumar, A., Q. A. Ansari, B. K. Kanaujia, and J. Kishor, "A novel ITI-shaped isolation structure placed between two-port CPW-fed dual-band MIMO antenna for high isolation," *AEÜ — Int. J. Electron. Commun.*, Vol. 104, 35–43, 2019.
17. Deng, J. Y., Z. J. Wang, J. Y. Li, and X. G. Li, "A dual-band MIMO antenna decoupled by a meandering line resonator for WLAN applications," *Microwave and Optical Technology Letters*, Vol. 60, No. 3, 759–765, 2018.
18. Leeladhar, M., R. K. Panigrahi, and M. V. Kartikeyan, "A 2×2 dual-band MIMO antenna with polarization diversity for wireless applications," *Progress In Electromagnetics Research C*, Vol. 61, 91–103, 2016.
19. Sarkar, D. and K. V. Srivastava, "Compact four-element SRR-loaded dual-band MIMO antenna for WLAN/WiMAX/WiFi/4G-LTE and 5G applications," *Electronics Letters*, Vol. 53, 1623–1624, 2017.
20. Luo, C.-M., J.-S. Hong, and M. Amin, "Mutual coupling reduction for dual-band MIMO antenna with simple structure," *Radioengineering*, Vol. 26, 51–56, 2017.
21. Jiang, W., Y. Cui, B. Liu, and W. Hu, "A dual-band MIMO antenna with enhanced isolation for 5G smartphone applications," *IEEE Access*, Vol. 7, 112554–112563, 2019.
22. Liu, Y., L. Yang, Y. Liu, J. Ren, J. Wang, and X. Li, "Dual-band planar MIMO antenna for WLAN application," *Microwave and Optical Technology Letters*, Vol. 57, No. 10, 2257–2262, 2015.
23. Desde, I., G. Bozdag, and A. Kustepeli, "Multi-band CPW-fed MIMO antenna for Bluetooth WLAN and WiMAX applications," *Microwave and Optical Technology Letters*, Vol. 58, No. 9, 2182–2186, 2016.
24. Ko, S. C. K. and R. D. Murch, "Compact integrated diversity antenna for wireless communications," *IEEE Transactions on Antennas and Propagation*, Vol. 49, 954–960, 2001.
25. Ramkrishnan, B. K. and G. N. Mulay, "Design of compact multiband pattern diversity antenna for WiMax, LTE and WLAN applications," *Microsyst Technol.*, Vol. 23, 1949–1960, 2017.
26. Mabrouk, I. B., L. Talbi, M. Nedil, and K. Hettak, "MIMO-UWB channel characterization within an underground mine gallery," *IEEE Transactions on Antennas and Propagation*, Vol. 60, No. 10, 4866–4874, 2012.
27. Ramachandran, A., S. Mathew, V. P. Viswanathan, M. Pezholil, and V. Kesavath, "Diversity-based four-port multiple input multiple output antenna loaded with interdigital structure for high isolation," *IET Microwaves Antennas Propag.*, Vol. 10, No. 15, 1633–42, 2016.
28. Chandel, R., A. K. Gautam, and K. Rambabu, "Tapered fed compact UWB MIMO-diversity antenna with dual band-notched characteristics," *IEEE Transactions on Antennas and Propagation*, Vol. 66, 1677–1684, 2018.
29. Kumar, A., A. Q. Ansari, B. K. Kanaujia, and J. Kishor, "High isolation compact four-port MIMO antenna loaded with CSRR for multiband applications," *Frequenz*, Vol. 72, 415–27, 2018.
30. Kumar, A., S. Kumar, Sinha, R. Sinha, and A. Choubey, "Dual circular slot ring triple-band MIMO antenna for 5G applications," *Frequenz*, Vol. 75, 91–100, 2021.